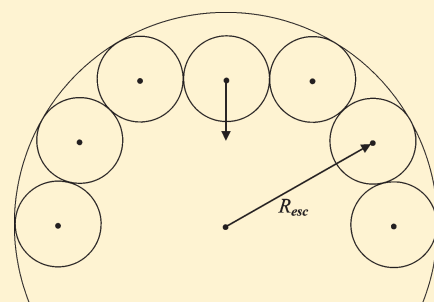


Modeling Collective Escape Processes for Nearly Jammed Systems

Frank H. Stillinger

Chemistry Department, Princeton University, Princeton, New Jersey 08544, United States

ABSTRACT: A simple kinetic model is introduced as an elementary contribution to understanding cooperative relaxation processes in condensed matter. This model involves n hard disks mutually trapped initially just inside an impenetrable circular boundary. Disk invasion of the interior of the system requires one of the disks to discover an exit passageway that only appears when the other disks collectively move out of the way. Cell approximations have been used to estimate the escape rate, in particular to show how that rate depends on n and on the increment of the boundary circle radius above the escape threshold.



I. INTRODUCTION

Kinetic processes in condensed phases display a wide diversity of observable time scales and measurable outcomes. These processes typically involve cooperative rearrangement motions of many of the constituent particles (atoms, ions, molecules). This contrasts starkly with the dynamical situation in dilute gas phases where conceptually simpler independent particle pair collisions dominate. It is hardly surprising that both experimental and theoretical research continue to be challenged in providing quantitative explanations for many condensed phase kinetic phenomena. In particular, relaxation processes in strongly supercooled liquids and in the glasses they form, as well as in other classes of amorphous solids, present many of these kinds of challenges to physical chemistry, chemical physics, and materials science.¹ The objective of the present paper is to describe, analyze, and interpret a relatively simple model that mimics some aspects of cooperative rearrangement processes in nearly jammed systems of hard particles. A recent review article covers some background information about the multidimensional configuration space description that is a natural representation for the hard particle phenomena to be considered.² Although the model described below involves oversimplification of physical reality, it does contain features that may serve to stimulate creation of more sophisticated approaches that are capable of producing deeper physical insights.

Attention focuses here on an elementary family of dynamical systems. Each of these contains $n \geq 6$ identical hard disks that are mutually trapped just inside the circumference of a large impenetrable circular boundary. Basic geometric details appear in the following section II. This is followed in section III with an analysis of the limited configuration space available to the disk set when the outer boundary radius lies in the trapping interval for a chosen n . With that background, section IV then describes the “escape gateway” that opens up once the boundary radius has been incremented slightly above the trapping threshold. Utilizing

those concepts, section V presents an estimate of the escape rate. Final remarks appear in section VI.

As a matter of passing interest, it may be worth noting that the dynamics of the model investigated here presents a rough analog to the Lindemann–Hinshelwood picture of unimolecular decomposition.³ In that description of chemical kinetics, following collision-induced energy activation, a fluctuation in vibrational intensity localized at a chemical bond in a molecule causes that bond to rupture. In the present model, a specific configurational fluctuation in the trapped cluster described below produces local disruption of an ordered initial structure, causing that initial structure subsequently to fall apart.

II. MODEL

Figure 1 presents the geometric starting point, for the specific case of $n = 12$ unit-diameter rigid disks placed just inside, and in contact with, a circular confining boundary. These disks are subject to strict nonoverlap restrictions among themselves, and with the encompassing circular boundary. As illustrated, the outer circle has the minimum radius $R_{\min}(n) + 1/2$ that is possible with the given number of disks, where $R_{\min}(n)$ in this configuration is the distance from the center of the bounding circle to the center of any one of the n disks. Simple trigonometry leads to the relation

$$R_{\min}(n) = 2^{-1/2} [1 - \cos(2\pi/n)]^{-1/2} \quad (1)$$

Although the set of n disks in this configuration can rotate as a whole around the interior of the boundary, they are otherwise

Special Issue: H. Eugene Stanley Festschrift

Received: May 26, 2011

Published: August 01, 2011

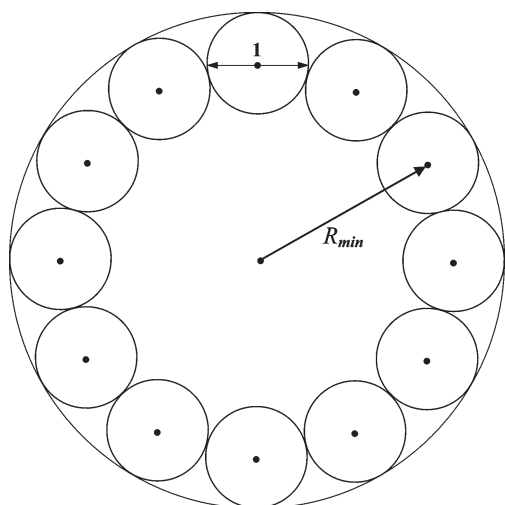


Figure 1. Cooperative radial trapping of twelve unit disks at a circular boundary. In the configuration shown, choice of the boundary radius $R_{\min} + 1/2$ forces all twelve disks to remain in contact with the boundary and with two neighboring disks. The disk arrangement can rotate as a rigid object around the boundary, but any inward displacements are prevented by nonoverlap constraints.

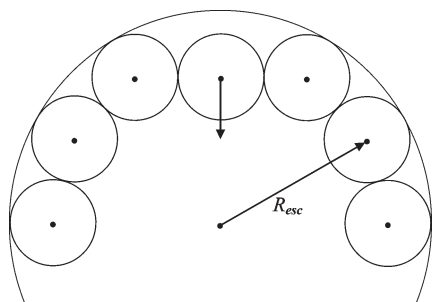


Figure 2. Critical inward escape configuration. This occurs when the boundary circle radius increases to $R_{\text{esc}} + 1/2$. For any one of the disks to slide inward past its two neighbors as indicated by the short arrow, all but that escapee must remain strictly in contact with the boundary and with neighbors.

trapped by their nonoverlap property and thus are unable to move into the interior of the large circular area.

Increasing the radius of the outer boundary by a small increment will allow the disks to move a limited amount relative to one another and relative to the boundary, in particular to eliminate all contacts. But unless that increased boundary radius has exceeded a threshold value $R_{\text{esc}}(n) + 1/2 > R_{\min}(n) + 1/2$ for escape, the disks will still be trapped radially by one another in the vicinity of the outer boundary, maintaining their same sequential order around the circumference. The geometric criterion that determines $R_{\text{esc}}(n)$ is illustrated in Figure 2. Before the increasing boundary radius attains that threshold value, displacing any one of the n disks to the maximum extent possible toward the system center (i.e., to the greatest inward separation from the circular boundary) forces the other $n - 1$ disks radially outward and into contact with the boundary and with one another. The escape threshold is finally attained when the chosen disk with maximum inward displacement and its two immediate neighbors have their centers along a straight line. As a result this disk can just slip past those neighbors, ultimately permitting unjamming of all disks,

Table 1. Numerical Values for the Minimum and Escape Radii R_{\min} and R_{esc} for Small Numbers n of Unit-Diameter Disks

n	$R_{\min}(n)$	$R_{\text{esc}}(n)$
6	1.000 000 000	1.072 356 268
7	1.152 382 436	1.197 605 338
8	1.306 562 965	1.338 166 692
9	1.461 902 200	1.485 469 731
10	1.618 033 989	1.636 385 973
11	1.774 732 766	1.789 477 262
12	1.931 851 652	1.943 983 369
13	2.089 290 734	2.099 462 579
14	2.246 979 604	2.255 640 000
15	2.404 867 173	2.412 335 361
16	2.562 915 448	2.569 425 450

which then are free to occupy the central portion of the large circular system. Although it is not possible to produce an explicit closed form for $R_{\text{esc}}(n)$, simple trigonometric analysis yields the following implicit relation (involving arc sine functions as asn) that can be used to evaluate that threshold quantity numerically:

$$\text{asn}\left[\frac{1}{R_{\text{esc}}(n)}\right] + (n-2) \text{asn}\left[\frac{1}{2R_{\text{esc}}(n)}\right] = \pi \quad (2)$$

Table 1 presents computed values for the two quantities $R_{\min}(n)$ and $R_{\text{esc}}(n)$ when the number of disks lies in the modest range $6 \leq n \leq 16$. It is also worth noting that eqs 1 and 2 can be used to develop asymptotic expansions applicable to the large- n regime. The results are the following:

$$R_{\min}(n) = \frac{1}{2}\left(\frac{n}{\pi}\right) + \frac{1}{12}\left(\frac{\pi}{n}\right) + \frac{7}{720}\left(\frac{\pi}{n}\right)^3 + O\left[\left(\frac{\pi}{n}\right)^5\right] \quad (3)$$

and

$$R_{\text{esc}}(n) = \frac{1}{2}\left(\frac{n}{\pi}\right) + \frac{1}{12}\left(\frac{\pi}{n}\right) + \frac{1}{2\pi}\left(\frac{\pi}{n}\right)^2 + \frac{7}{720}\left(\frac{\pi}{n}\right)^3 + O\left[\left(\frac{\pi}{n}\right)^4\right] \quad (4)$$

These expressions imply that the trapping interval for the boundary radius has a large- n shrinkage obeying the asymptotic form

$$R_{\text{esc}} - R_{\min} = \frac{\pi}{2n^2} + O\left[\left(\frac{\pi}{n}\right)^4\right] \quad (5)$$

III. AVAILABLE CONFIGURATION SPACE

If the radius $R + 1/2$ of the bounding circle is sufficiently large, the $2n$ -dimensional configuration space available to the unit-diameter disks within that boundary is connected. In other words, any one arrangement with disk centers at $\mathbf{r}_1, \dots, \mathbf{r}_n$ that does not violate overlap conditions can be continuously deformed into any other nonoverlap arrangement $\mathbf{r}_1', \dots, \mathbf{r}_n'$ along a path whose entirety also avoids overlaps. However, as R declines to a value just above $R_{\text{esc}}(n)$, this connected manifold begins to

extrude a group of geometrically equivalent small portions that correspond to clustering of the n disks just inside the boundary circumference. This clustering can occur in $(n - 1)!$ distinct ways, depending on the circumferential arrangement order adopted by the n disks. When R declines through $R_{\text{esc}}(n)$, very narrow connection tubes (whose details are analyzed below) close up, disconnecting the $(n - 1)!$ extruded pieces from the dominant available region and isolating them from one another. Continued reduction in R causes shrinkage of the $2n$ -dimensional content of each of the boundary-clustering regions, all $(n - 1)!$ of which simultaneously vanish at $R = R_{\text{min}}(n)$.

Although it is not a matter of primary concern in the following, it should be noted in passing that if n is sufficiently large this kind of disconnection process for the available configuration space can in principle repeat upon further decline in R . It is possible for $n - 1$ disks to become trapped along the circular boundary, while one disk enjoys motion freedom within the interior of the circular boundary. Subsequently, provided that n is sufficiently large, $n - 2$ disks could be boundary-trapped at even smaller R with 2 disks free to move in the interior, followed by further analogous disconnection events. This sequence of disconnections and jamming processes eventually terminates as boundary radius $R + 1/2$ shrinks toward the minimum possible value that can accommodate n disks jammed within its interior.⁴

The natural way to specify the n disk positions is to use polar coordinates whose origin is at the center of the encompassing boundary circle. These coordinates will be written as r_j, θ_j , respectively for the radial distance and polar angle of disk j ($1 \leq j \leq n$). For the moment attention will focus on disk trapping resulting from $R_{\text{min}}(n) < R < R_{\text{esc}}(n)$, with restriction to the disk arrangement for which index j increases counterclockwise within the outer boundary circumference. There are $2n$ nonoverlap constraints that maintain the trapping situation. The first n are simply due to the boundary confinement:

$$r_j \leq R \quad (1 \leq j \leq n) \quad (6)$$

The remaining n constraints are the disk–pair nonoverlap conditions:

$$|\mathbf{r}_{j+1}(r_{j+1}, \theta_{j+1}) - \mathbf{r}_j(r_j, \theta_j)| \geq 1 \quad (1 \leq j \leq n) \quad (7)$$

with the convention that disk index $n + 1 \equiv 1$. When this last set of constraints is expressed explicitly in terms of the polar coordinates, one obtains

$$r_j^2 + r_{j+1}^2 - 2r_j r_{j+1} \cos(\theta_{j+1} - \theta_j) \geq 1 \quad (1 \leq j \leq n) \quad (8)$$

Inequalities (6) and (8) uniquely define the isolated region in the $2n$ -dimensional configuration space for the boundary-trapped disk arrangement. The corresponding equalities define the $2n$ bounding hypersurfaces for the trapping region.

As R approaches $R_{\text{min}}(n)$ from above, the $2n$ constraining inequalities squeeze the isolated region to zero size in all but one degree of freedom, specifically the one associated with simultaneous circumferential rotation of the full disk set. To describe this asymptotic limit in detail, it is convenient to set

$$R = R_{\text{min}}(n) + \Delta \quad (9)$$

and for the trapped disk coordinates

$$\begin{aligned} r_j &= R - \delta_j \equiv R_{\text{min}}(n) + \Delta - \delta_j \quad (1 \leq j \leq n) \\ \theta_j &= \theta_1 + [2\pi(j-1)/n] + \varepsilon_j \quad (2 \leq j \leq n) \end{aligned} \quad (10)$$

As the second of the expressions 10 indicates, by measuring $j - 1$ of the polar angles relative to θ_1 the global rotation mode becomes isolated from the details of disk relative displacements that produce the vanishing of the region at $\Delta = 1$. This directs attention to the $(2n - 1)$ -dimensional subspace of allowed configurations that is orthogonal to coordinate θ_1 , and which the $2n$ bounding hypersurfaces force to collapse to a point at $R = R_{\text{min}}(n)$ in that subspace.

After linearization in terms of the vanishingly small quantities Δ, δ_j , and ε_j , the constraint conditions in eqs 6 and 8 appear as follows ($1 \leq j \leq n$):

$$\begin{aligned} \delta_j &\geq 0, \quad 2\Delta - \delta_{j+1} - \delta_j \\ &+ 2^{-1/2}[1 - \cos(2\pi/n)]^{-3/2} \sin(2\pi/n)(\varepsilon_{j+1} - \varepsilon_j) \geq 0 \end{aligned} \quad (11)$$

These $2n$ linear constraints on the δ_j and ε_j define a simplex polytope in the $(2n - 1)$ -dimensional subspace, i.e., a convex bounded region enclosed by the minimum possible number of flat hyperfaces.⁵ The fact that inequalities (11) are homogeneous with degree unity implies that to be inside the simplex the coordinates $\delta_1, \dots, \delta_n, \varepsilon_2, \dots, \varepsilon_n$ must scale as the first power of the control parameter Δ . This in turn implies that the $(2n - 1)$ -dimensional content of the simplex in the small- Δ limit must have the form

$$C(n)\Delta^{2n-1} \quad (12)$$

where $C(n) > 0$ will depend on n as indicated. When the remaining rotational degree of freedom is included, the small- Δ limit of the content for any one of the $(n - 1)!$ separated trapping regions will be

$$2\pi C(n) R_{\text{min}}(n) \Delta^{2n-1} \quad (13)$$

This expression represents the leading-order term in an expression for the content $K(\Delta, n)$ of each trapping region when $R_{\text{min}}(n) \leq R \leq R_{\text{esc}}(n)$:

$$K(\Delta, n) = 2\pi C(n) R_{\text{min}}(n) \Delta^{2n-1} + O(\Delta^{2n}) \quad (14)$$

When R is close to, but slightly less than, its trapping upper limit $R_{\text{esc}}(n)$, the trapping-region content expressed by $K(\Delta, n)$, compared to its small- Δ limiting simplex form, is enhanced slightly by bounding hypersurface curvature effects. These effects create the precursor of n narrow escape channels into the large nontrapped portion of available configuration space. One basic measure of this developing protuberance is how close to the system center one of the disks, e.g., disk number k , can approach as a function of R . By comparison with the $R = R_{\text{esc}}(n)$ threshold illustrated in Figure 2, the arrangement with the minimum possible distance r_k when R is slightly less than $R_{\text{esc}}(n)$ would have the center of disk k located slightly above the line connecting centers of its two contact neighbors $k - 1$ and $k + 1$. As mentioned earlier, all disks except k are then forced outward into contact with the large bounding circle and into contact with one another. Denote this R -dependent minimum distance available to disk k by $s(R, n)$. It is straightforward to derive the following quadratic equation which

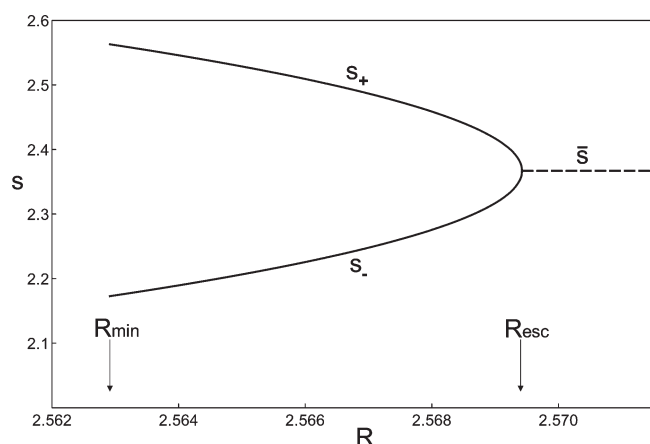


Figure 3. Outer (s_+) and inner (s_-) solutions of eq 15 vs R for $n = 16$ unit disks. The dashed curve shows $\bar{s} = (s_+ + s_-)/2$, which specifies the radial location of the exit gateway when $R > R_{\text{esc}}(n)$.

determines that distance:

$$s^2 - [2R \cos \psi(R, n)]s + R^2 - 1 = 0 \quad (15)$$

in which the quantity $\psi(R, n)$ involves an arc cosine function acs :

$$\psi(R, n) = \pi - \left(\frac{n-2}{2} \right) \text{acs} \left(1 - \frac{1}{2R^2} \right) \quad (16)$$

The formal solution pair is

$$s(R, n) = R \{ \cos \psi(R, n) \pm [\cos^2 \psi(R, n) - 1 + R^{-2}]^{1/2} \} \quad (17)$$

the upper sign is the relevant choice for disk trapping, while the lower sign corresponds to a “mirror image” alternative disk- k position that also contacts the two neighbors but has its center below the straight line segment connecting the centers of those neighbors.

Figure 3 provides a graph of $s(R, n)$ vs R for $n = 16$. Both the outer (s_+) and the inner (s_-) branches from eq 17 are shown, with only the former directly relevant to the impending escape process. The diverging rates of change of s_+ and s_- as R approaches R_{esc} are a result of hypersurface curvature at the boundary of the trapping region. Qualitatively similar results would be obtained for other n values.

IV. ESCAPE PROCESS

The main objective of this investigation is to analyze the escape rate from the multidimensional region of boundary-trapped configurations when R slightly exceeds the threshold value $R_{\text{esc}}(n)$. This radial excess will be denoted by

$$\Delta^* = R - R_{\text{esc}}(n) = \Delta + R_{\text{min}}(n) - R_{\text{esc}}(n) \quad (18)$$

The escape rate can be inferred from an ensemble of nominally identical systems whose initial configurations ($t = 0$) are uniformly distributed within one of the extrusion regions, with all n disks of mass m subject to a Maxwell–Boltzmann velocity distribution for absolute temperature T . Because each ensemble member will be regarded as isolated, its subsequent dynamics ($t > 0$) conserves both energy and angular momentum. The relevant part of the ensemble’s time evolution can be summarized by the time-dependent probability $P(t)$ that escape has occurred.

With this convention one has

$$\begin{aligned} P(0) &= 0 \\ P(+\infty) &= 1 \end{aligned} \quad (19)$$

The latter of these relations is based on the supposition that the disk system collisional dynamics within the trapping region is ergodic, owing to the various relative orientations of the bounding hypersurfaces, as well as to their small curvatures. The ensemble-average mean lifetime of the temporarily trapped disk arrangements prior to escape would be

$$\tau = \int_0^\infty [1 - P(t)] dt \quad (20)$$

Of course with equal probability in the ensemble any one of the n disks could be the one to lead the way to escape.

To complete the definition of $P(t)$, it is necessary to specify precisely what disk configurations amount to the escape “gateway” when $\Delta^* > 0$. This involves identifying the location of the narrowest part of the escape channel. For present purposes this location will be identified as the radial coordinate r_l for the first-escaping disk, e.g., l , declining (i.e., passing inward) through the value:

$$\begin{aligned} r_l &= \bar{s}(R, n) \\ &= R \cos \psi(R, n) \\ &= [R_{\text{esc}}(n) + \Delta^*] \cos \psi[R_{\text{esc}}(n) + \Delta^*, n] \end{aligned} \quad (21)$$

Note that this choice is formally the average of the two solutions for $s(R, n)$ presented in eq 17 above. This is the position at which a disk hypothetically would have to experience the greatest shrinkage in size to slip past its two unit-diameter neighbors when $\Delta^* < 0$, but which functionally smoothly continues to $\Delta^* > 0$. Alternatively, this can be identified as the radial location of the midpoint connecting centers of disks $l - 1$ and $l + 1$ when all but disk l are forced against the outer bounding circle, and forced into contact with one another. Figure 3 shows the R dependence of $\bar{s} = (s_+ + s_-)/2$ for $n = 16$ as a dashed curve.

The trapping region content $K(\Delta, n)$ shown earlier in eq 14 referred only to $R_{\text{min}} \leq R \leq R_{\text{esc}}$. However, it is now useful to extend the definition of this symbol to refer to the content of one of the extruded trapping regions for $R > R_{\text{esc}}$ (i.e., $\Delta^* > 0$) by appending to the constraints in eqs 6 and 8 the escape gateway conditions:

$$r_j \geq \bar{s}(R, n) \quad (1 \leq j \leq n) \quad (22)$$

This increases the number of bounding hypersurfaces defining $K(\Delta, n)$ from the previous $2n$ to $3n$. Provided that the increment Δ^* of R above R_{esc} is not too large, the escape gateways for each of the n disks remain geometrically separated from each other. That is, if prior to any escape one of the n disks were to move radially inward to \bar{s} , the other $n - 1$ disks would be constrained by the nonoverlap conditions to remain at radial distances greater than \bar{s} . Let $L(\Delta^*, n)$ stand for the $(2n - 1)$ -dimensional manifold of configurations for which one specific disk is at the escape gateway, while the $n - 1$ others still have $r_j > \bar{s}$. As was the case for $K(\Delta, n)$, this manifold also includes collective angular rotation of the full disk set inside the large circular boundary. The set of n such manifolds with total measure $nL(\Delta^*, n)$ constitutes the set of “leaks” through which $K(\Delta, n)$ loses its initial occupancy, as described by $P(t)$, eqs 19 and 20.

Prior to an escape event for a given ensemble member, a $K(\Delta, n)$ region contains a single $2n$ -dimensional configuration point, but after escape it is empty. Formally speaking, that escape event causes the multidimensional interior number density $\rho(t)$ for $K(\Delta, n)$ to drop discontinuously from $1/K(\Delta, n)$ to zero. Upon averaging over the postulated ensemble of systems, the time dependence of the $K(\Delta, n)$ -contained number density would be described as

$$\langle \rho(t) \rangle = [1 - P(t)]/K(\Delta, n) \quad (23)$$

This quantity will decline monotonically with time at a rate determined by configurational point leakage across the n exit manifolds each of measure $L(\Delta^*, n)$. The expected average current across these gateways depends on the hyperarea of the n gateways, and on the exit current per unit hyperarea. At time t the latter is determined by the presumed Maxwell–Boltzmann velocity distribution, and the average number density. As a result one has

$$\begin{aligned} d\rho(t)/dt &= nL(\Delta^*, n)\langle \rho(t) \rangle \\ &\times \int_0^\infty (2\pi mk_B T)^{-1/2} v \exp(-v^2/2mk_B T) dv \end{aligned} \quad (24)$$

where k_B is Boltzmann's constant, and v represents the velocity component from the full hyperspherically symmetric Maxwell–Boltzmann distribution that is normal to the gateway hypersurface. By carrying out the velocity integration and inserting the expression for mean density from eq 23, one finds that eq 24 is equivalent to the following differential equation:

$$\frac{d[1 - P(t)]}{dt} = - \left(\frac{mk_B T}{2\pi} \right)^{1/2} \frac{nL(\Delta^*, n)}{K(\Delta, n)} [1 - P(t)] \quad (25)$$

Upon integrating this relation subject to the conditions in eqs 19, one obtains the simple result

$$P(t) = 1 - \exp(-t/\tau) \quad (26)$$

where

$$\tau = \left(\frac{mk_B T}{2\pi} \right)^{1/2} \frac{nL(\Delta^*, n)}{K(\Delta, n)} \quad (27)$$

is the estimated mean residence lifetime in the trapping region, eq 20.

V. ESCAPE RATE ESTIMATE

The next step requires evaluating, or at least estimating, the magnitudes of the content measures $K(\Delta, n)$ and $L(\Delta^*, n)$ for small escape rates, i.e., for small Δ^* . The specific objective is to generate an expression for lifetime τ that explicitly indicates its dependence on n and Δ^* . For this purpose, a self-consistent “cell approximation” will be utilized for the ring of n disks in the vicinity of the bounding circle. Although such an approximation may not be very precise for either quantity $K(\Delta, n)$ or $L(\Delta^*, n)$ separately, the corresponding errors should be of comparable relative magnitude, and hence tend to cancel in their ratio that is required to determine τ , eq 27.

First consider the trapping situation, $R_{\min} < R < R_{\text{esc}}$. Introduce a “standard” configuration of the n disks for which

$$\begin{aligned} \delta_j &= \hat{\delta} \quad (1 \leq j \leq n) \\ \varepsilon_j &= 0 \quad (2 \leq j \leq n) \end{aligned} \quad (28)$$

Nonoverlap restrictions require $0 \leq \hat{\delta} \leq \Delta$. That is, in this standard arrangement the n disks have a common radial distance and a regular polar angle separation. Then if any one of the disks is allowed to wander from its own standard position while the remaining $n - 1$ remain fixed, that one disk will be confined to a small isosceles triangle (in leading order in the unjamming parameter Δ). Simple geometry leads to the conclusion that the area of that triangle of single-disk displacements will be

$$\Delta^2 \tan(2\pi/n) \quad (29)$$

which in the leading order considered is independent of $\hat{\delta}$. A feasible cell approximation for $K(\Delta, n)$ can then be composed multiplicatively of $n - 1$ triangle areas (29), and the radial and full circumferential motion of disk $j = 1$:

$$\begin{aligned} K(\Delta, n) &\approx [\Delta^2 \tan(2\pi/n)]^{n-1} \cdot \Delta \cdot 2\pi R_{\min}(n) \\ &= 2\pi R_{\min}(n) \Delta^{2n-1} [\tan(2\pi/n)]^{n-1} \end{aligned} \quad (30)$$

To produce a corresponding cell approximation for $L(\Delta^*, n)$, first observe that the bounding circumference for the centers of the $n - 1$ disks that are not at the escape threshold has increased from $2\pi R_{\text{esc}}$ to $2\pi R_{\text{esc}} + \Delta^*$ as Δ^* has increased from zero. This amounts to $2\pi\Delta^*/(n - 1)$ per disk, a distance that can serve effectively as a tangential direction base for a cell-approximation displacement triangle. The radial-direction height of such a triangle can be reasonably estimated as Δ^* itself, thus leading to triangle area $\pi(\Delta^*)^2/(n - 1)$. In analogy to the form shown in eq 30 for $K(\Delta, n)$, the $L(\Delta^*, n)$ estimate is built up from the product of $n - 1$ disk displacement triangle factors, and the circular rotational freedom for the single disk at the escape threshold:

$$\begin{aligned} L(\Delta^*, n) &\approx [\pi(\Delta^*)^2/(n - 1)]^{n-1} \cdot 2\pi\bar{s}[R_{\text{esc}}(n) + \Delta^*, n] \\ &\approx 2\pi^n (n - 1)^{1-n} (\Delta^*)^{2n-2} \bar{s}[R_{\text{esc}}(n), n] \end{aligned} \quad (31)$$

The latter form shown retains only the leading order in the small parameter Δ^* , which is sufficient for present purposes.

Substituting the last two results into eq 27 finally yields the desired estimate for the escape lifetime:

$$\tau \approx \left(\frac{mk_B T}{2\pi} \right)^{1/2} \left\{ \frac{\pi^{n-1} n (n - 1)^{1-n} \bar{s}[R_{\text{esc}}(n), n] (\Delta^*)^{2n-2}}{R_{\min}(n) [\tan(2\pi/n)]^{n-1} \Delta^{2n-1}} \right\} \quad (32)$$

To partially clarify the implications of this form for τ , it is useful first to restrict attention to its leading order in escape parameter Δ^* . This involves replacing Δ by its value at the escape threshold:

$$\Delta_{\text{esc}}(n) = R_{\text{esc}}(n) - R_{\min}(n) \quad (33)$$

the large- n behavior of which was specified earlier in eq 5. Further simplification then emerges by extracting the large- n asymptotic limit of this leading Δ^* -order expression for τ , utilizing the simplification:

$$\lim_{n \rightarrow \infty} \bar{s}[R_{\text{esc}}(n), n]/R_{\text{esc}}(n) = 1 \quad (34)$$

This leads specifically to the small- Δ^* result:

$$\tau \sim \left(\frac{mk_B T}{2\pi} \right)^{1/2} \left(\frac{2^n e n^{4n-1}}{\pi^{2n-1}} \right) (\Delta^*)^{2n-2} \quad (35)$$

An alternative version of this last expression involves scaling the escape parameter Δ^* by Δ_{esc} :

$$\tau \sim \left(\frac{mk_{\text{B}}T}{2\pi}\right)^{1/2} \left(\frac{en^3}{2^{n-2}\pi}\right) \left(\frac{\Delta^*}{\Delta_{\text{esc}}(n)}\right)^{2n-2} \quad (36)$$

This scaling converts the coefficient in eq 35 from a form that is strongly divergent as $n \rightarrow +\infty$ to a strongly convergent form. However, the key characteristic in either case is the power $2n - 2$ for Δ^* , indicating the aggravation with increasing n of the initial difficulty that the dynamical system has in locating one of the n exit channels as those channels just begin to open for escape.

VI. FINAL REMARKS

Although the family of models introduced here to illustrate trapping and escape kinetics is conceptually simple, it illustrates at least some aspects of the collective character of relaxation processes that occur in condensed matter phases. The rather elementary “cell approximations” invoked to determine the qualitative implications of those models near their escape thresholds no doubt could be improved quantitatively. One possibility would invoke a reversible isothermal process in a numerical simulation wherein the disk repulsive potentials are continuously “turned on”, starting with an ideal gas of n particles confined radially to $R_{\text{min}}(n) \leq r_j \leq R$ or to $\bar{s} \leq r_j \leq R$. The respective entropies for these processes could then be converted to accurate values for K and L , and thus for the lifetime τ .

If the radius of the bounding circle is sufficiently large so that $\Delta^* > 0$, then time reversibility permits the inverse of the escape scenario to occur. In other words it is dynamically possible for a set of n hard disks that initially occupy the center of the system to reverse the escape scenario. Such an improbable event would require a collision sequence causing the n disks spontaneously to form one of the $(n - 1)!$ rings just inside the large circular boundary. That involves motion of the $2n$ -dimensional configuration point into, and through, one of the narrow escape channels and thus into the interior of one of the small $K(\Delta, n)$ regions. The appearance of such an unusual return event can be described by an ensemble-average time to occurrence τ_{ret} . It would be related to the mean escape time τ by a factor determined by the ratio of contents for the untrapped portion of configuration space, $M(\Delta, n)$, to that of all $(n - 1)!$ trapping regions $K(\Delta, n)$:

$$\tau_{\text{ret}}(\Delta^*) = \left[\frac{M(\Delta, n)}{(n - 1)!K(\Delta, n)}\right] \tau(\Delta^*) \quad (\Delta^* > 0) \quad (37)$$

The trapping geometry and escape kinetics described in the previous sections for single rings of hard disks can in principle be extended to wider families of hard-particle models. One avenue for generalization in two dimensions would be based on the geometry of “curved hexagonal” packings of identical hard disks inside a large circular boundary.⁶ These arrangements fill the interior of the bounding circle with jammed concentric rings of particles, where those rings involve fewer and fewer disks as the center (a single disk) is approached. Evidently the central disk and the innermost particle rings can be removed, while those remaining rings continue to be trapped against the outer boundary by nonoverlap constraints. For a chosen number of remaining rings of disks it should be possible to identify the corresponding R_{min} and R_{esc} parameters, referring as above to the radial positions of the outermost ring of disks when they are in

contact with the boundary at jamming, and at the escape threshold for the innermost remaining ring.

Three dimensional versions of the present simple model are also possible. A conceptually straightforward example would involve 12 identical hard spheres in an icosahedral arrangement, pressed against a spherical impenetrable boundary by their own nonoverlap constraints. Again it is feasible to identify numerically the $R_{\text{min}}(12)$ and $R_{\text{esc}}(12)$ for this version. Whether there might be other similar three-dimensional structures with larger numbers n of trapped hard spheres remains an unexplored possibility. In particular, it is currently unknown if the “curved hexagonal” family of disk configurations⁶ has a three-dimensional extension.

ACKNOWLEDGMENT

The author gratefully acknowledges preliminary molecular dynamics simulations produced by Dr. Boris D. Lubachevsky for the model described in this paper. The author also thanks D. K. Stillinger for creating Figures 1–3.

REFERENCES

- (1) (a) Williams, M. L.; Landel, R. F.; Ferry, J. D. *J. Am. Chem. Soc.* **1955**, *77*, 3701. (b) Debenedetti, P. G. *Metastable Liquids*; Princeton University Press: Princeton, NJ, 1996. (c) Angell, C. A.; Ngai, K. L.; McKenna, G. B.; McMillan, P. F.; Martin, S. W. *J. Appl. Phys.* **2000**, *88*, 3113. (d) Ediger, M. D. *Annu. Rev. Phys. Chem.* **2000**, *51*, 99. (e) Wales, D. J. *Energy Landscapes*; Cambridge University Press: Cambridge, England, 2003. (f) Heuer, A. *J. Phys.: Condens. Matter* **2008**, *20*, 1.
- (2) Torquato, S.; Stillinger, F. H. *Rev. Mod. Phys.* **2010**, *82*, 2633.
- (3) Levine, R. D. *J. Chem. Phys.* **1968**, *48*, 4556.
- (4) Graham, R. L.; Lubachevsky, B. D.; Nurmela, K. J.; Östergård, P. R. J. *Discrete Math.* **1998**, *181*, 139.
- (5) Grünbaum, B. *Convex Polytopes*; Interscience Publishers: New York, 1967.
- (6) Lubachevsky, B. D.; Graham, R. L. *Discrete Comput. Geom.* **1997**, *18*, 179.